

**PAULINA KOMAR¹, PATRYCJA ŚPIEWAK¹,
MARCIN GĘBSKI^{1,2}, JAMES A. LOTT², MICHAŁ WASIAK¹**

¹Institute of Physics, Lodz University of Technology, ul. Wólczajska 219,
90-924 Łódź, Poland, e-mail: paulina.komar@p.lodz.pl

²Institute of Solid State Physics and the Center of Nanophotonics,
Technical University of Berlin, D-10632 Berlin, Germany

CURRENT DEPENDENCE OF RESISTANCES AND CAPACITANCES IN A VERTICAL-CAVITY SURFACE-EMITTING LASER

Based on the model of impedance and modulation time constants for vertical-cavity surface-emitting lasers (VCSELs) we study the resistances and capacitances of an equivalent circuit as a function of the current flowing through the VCSEL. We observe reduction of some components of the resistance and the capacitance, as well as the modulation time constants for increasing current.

Keywords: VCSEL, high-frequency modulation, capacitance, modelling of semiconductor lasers.

1. INTRODUCTION

In recent years, the vertical-cavity surface-emitting lasers (VCSELs) are constantly gaining importance as transmitters in short-range optical data transfer due to their low cost, small size, low power consumption, and good quality of the emitted beam [1-3]. While being used as the light source for optical data communication, the VCSEL is set at a fixed bias current and modulated with a high-frequency voltage. At the modulation frequencies of tens of GHz, enabling high bandwidth data transmission, it becomes important to identify and investigate how the electrical capacitances and resistances present in the system depend on operation parameters of a laser to assure error-free operation [4-5].

2. SIMULATION MODEL

The simulations of the temperature and electrical potential distributions inside semiconductor lasers are performed based on the self-consistent thermal-electrical model developed by the Photonics Group at the Lodz University of Technology [6-7]. The investigations presented in this article are based in particular on an extension of this model, *i.e.* the numerical model of impedance developed by Wasiak *et al.* [5]. The main idea of this model is a division of the entire laser into areas whose borders have the same potential. Knowing the equipotential surfaces one can connect these areas in series while building an equivalent circuit.

A scheme of the investigated laser and its equivalent electrical circuit are presented in Fig. 1(a) and 1(b), respectively. The VCSEL structure consists of a p-type and n-type distributed Bragg reflectors (DBRs), spaced by a p-i-n junction (drawn in green), *i.e.* the undoped material between two doped semiconductors. We consider also two oxide layers – one on the p-type side (drawn in purple) and one on the n-type side (drawn in blue) of the junction. As one can find equipotential surfaces between these layers, one can create an equivalent circuit composed of capacitances (C) and resistances (R) due to oxide layer on the p-type side (with subscript oxp), due to junction layer (with subscript j), and due to oxide layer on the n-type side (with subscript oxn).

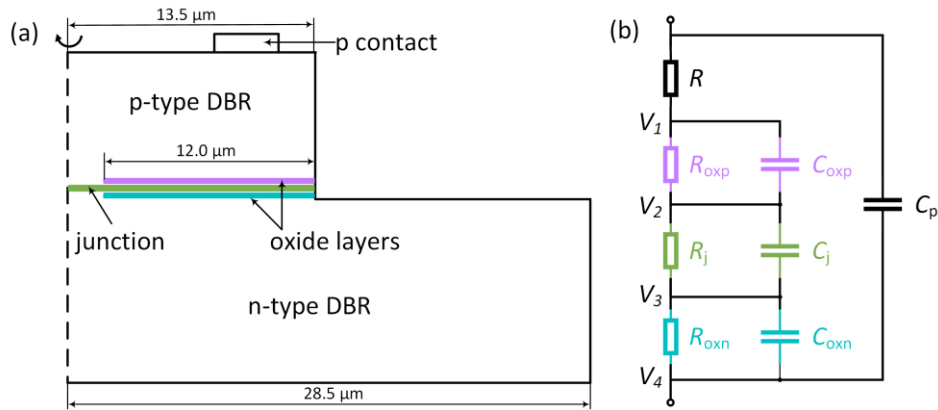


Fig. 1. (a) A scheme of the VCSEL structure employed to simulations. The thicknesses of the oxide layers and the active region (junction) are not drawn to scale. (b) An equivalent circuit of a VCSEL with oxide layers on both sides of a junction. Description of symbols is given in the text

The resistance of the remaining semiconductor material is labelled with R , whereas the capacitance of the insulating materials surrounding the laser is represented by C_p .

It is crucial to mention that the physical borders between the layers (*e.g.* the oxide layer on the p-type side and the junction) do not overlap with the equipotential surfaces that are used for definition of the equivalent circuit. One can clearly see this situation on maps presented in Fig. 2, where the equipotential lines are drawn in black on top of the VCSEL zoomed on the active region (yellow) and the oxide layers located on its both sides (purple). Thus, area that is located between potentials V_1 and V_2 (compare Figs. 1(b) and 2) is considered as the resistance R_{oxp} and capacitance C_{oxp} , between potentials V_2 and V_3 corresponds to the junction (R_j and C_j), whereas between V_3 and V_4 is treated as the resistance R_{oxn} and capacitance C_{oxn} due to oxide layer on the n-type side.

3. SIMULATION RESULTS

The simulations were performed for a structure [1-3] schematically presented in Fig. 1(a), for which the aperture diameter is equal to 3 μm , the diameter of the p-type DBR is equal to 27 μm , and the diameter of the n-type DBR is equal to 57 μm . The numerical studies of the temperature and potential distributions were executed for four fixed values of voltage ($U = 1.9, 2.1, 2.5, 3.0$ V) applied to the contacts of the laser. The performed calculations allowed for determination of the values of the current flowing through the VCSEL, all the resistances and capacitances in the model, and the maximum value of the modulation time constant.

The values of the resistances calculated as a function of the current flowing through the VCSEL are presented in Fig. 3. Due to the fact that R_j is the differential resistance of the junction, one can observe a strong decrease of its value as a function of current. In contrast, R_{oxn} and R are almost independent on I . The highest values of the resistance were obtained for oxidation layer on the p-type side due to lower electrical conductivity of p-type semiconductors used for construction of the DBR. The total resistance (sum of all discussed resistances) of the VCSEL as well as the R_{oxp} are decreasing for increasing current, what is in agreement with experimental observations [1].

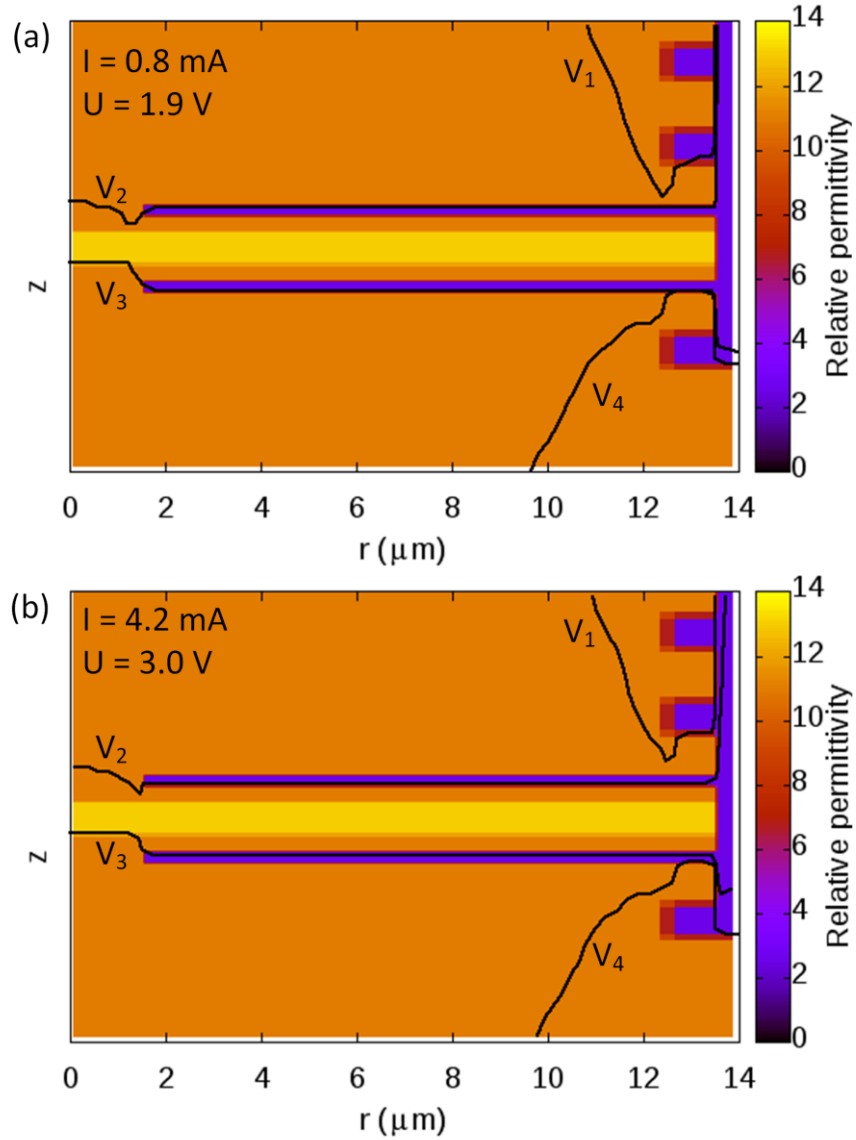


Fig. 2. The equipotential lines drawn on top of the VCSEL structure for (a) current $I = 0.8 \text{ mA}$, voltage $U = 1.9 \text{ V}$ and (b) current $I = 4.2 \text{ mA}$, voltage $U = 3.0 \text{ V}$. Individual layers may be distinguished based on their relative permittivity. The maps show a zoom on the active region and the oxide layers located on its both sides

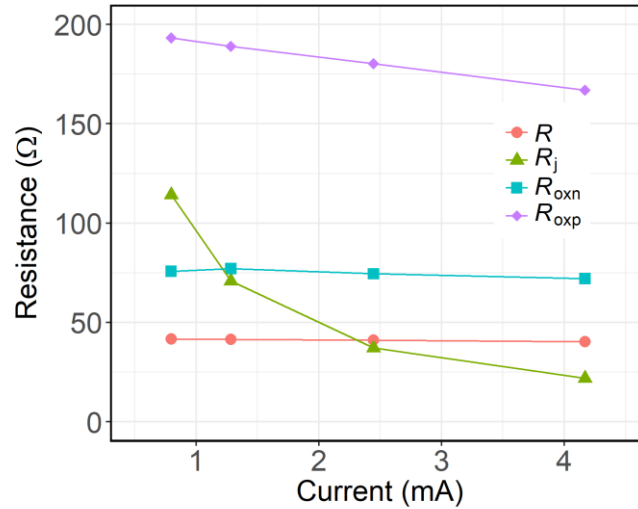


Fig. 3. Calculated values of resistances present in an equivalent circuit as a function of the current flowing through the VCSEL. The lines are guides to the eye

The calculated values of capacitances as a function of the current are shown in Fig. 4. The capacitances of the junction C_j and the dielectric material surrounding the laser C_p are almost independent on the current. On the other hand, one can notice significant decrease of the capacitances due to oxide layers. That is due to the fact that change of the applied voltage leads to a change of the distribution of the potentials $V_1 - V_4$. For higher voltage (see Fig. 2(b)), the potentials V_2 and V_3 move towards the junction as compared to the lower voltage (see Fig. 2(a)). Therefore, the effective oxidation thickness increases for increasing voltage (and also the current), what leads to the decrease of the capacitance.

Based on the employed model of capacitance one can also calculate the modulation time constants τ . In Fig. 5, we present the maximum value of τ from among three calculated time constants. As clearly visible, the value of the modulation time constant decreases for increasing current. Therefore, for higher current the VCSEL may be modulated with higher frequency enabling quicker data transfer.

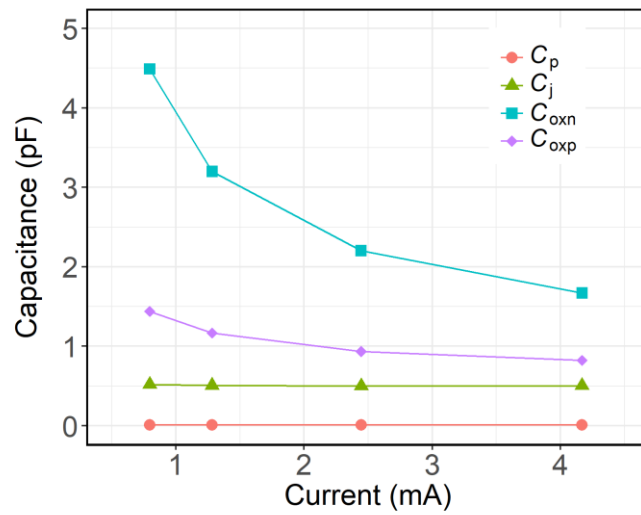


Fig. 4. Calculated values of capacitances present in an equivalent circuit as a function of the current flowing through the VCSEL. The lines are guides to the eye

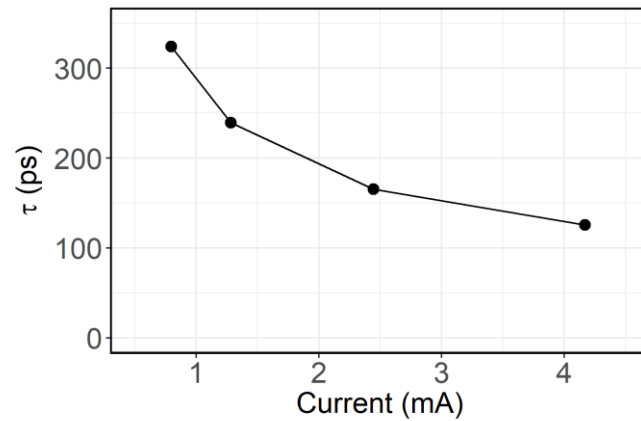


Fig. 5. Modulation time constant as a function of the current flowing through the VCSEL. The line is a guide to the eye

4. CONCLUSIONS

Employing the model of impedance for VCSELs we have calculated the resistances and capacitances of a laser as a function of the current. We observe that the differential resistance as well as capacitances associated with the oxide layers are decreasing for increasing current. That leads to a decrease of modulation time constant for increasing I , enabling modulation with higher frequency and faster data transfer.

ACKNOWLEDGMENT

We gratefully acknowledge financial support by NCN 2016/21/B/ST7/03532.

REFERENCES

- [1] Li H., Lott J.A., Wolf P., Moser P., Larisch G., Bimberg D. 2015. Temperature-dependent impedance characteristics of temperature-stable high-speed 980 nm VCSELs. *IEEE Photon. Technol. Lett.* 27:832-835.
- [2] Li H., Wolf P., Moser P., Larisch G., Lott J.A., Bimberg D. 2014. Temperature-stable 980 nm VCSELs for 35 Gb s⁻¹ operation at 85 °C with 139 fJ/bit dissipated heat. *IEEE Photon. Technol. Lett.* 26:2349-2352.
- [3] Moser P., Lott J.A., Larisch G., Bimberg D. 2015. Impact of the oxide-aperture diameter on the energy-efficiency, bandwidth, and temperature stability of 980 nm VCSELs. *J. Lightwave Technol.* 33:825-831.
- [4] Ou Y., Gustavsson J.S., Westbergh P., Haglund Å., Larsson A., Joel A. 2009. Impedance characteristics and parasitic speed limitations of high-speed 850 nm VCSELs. *IEEE Photon. Technol. Lett.* 21:1840-1842.
- [5] Wasiak M., Śpiewak P., Moser P., Walczak J., Sarzała R.P., Czyszanowski T., Lott J.A. 2016. Numerical model of capacitance in vertical-cavity surface-emitting lasers. *J. Phys. D: Appl. Phys.* 49:175104.
- [6] Piskorski Ł., Sarzała R.P., Nakwaski W. 2007. Self-consistent model of 650 nm GaInP/AlGaInP quantum-well vertical-cavity surface-emitting diode lasers. *Semicond. Sci. Technol.* 22:593-600.
- [7] Xu D., Tong C., Yoon S.F., Fan W., Zhang D.H., Wasiak M., Piskorski Ł., Gutowski K., Sarzała R.P., Nakwaski W. 2009. Room-temperature continuous-wave operation of the In(Ga)As/GaAs quantum-dot VCSELs for the 1.3 μm optical-fibre communication. *Semicond. Sci. Technol.* 24:055003.

PRĄDOWA ZALEŻNOŚĆ REZYSTANCJI I POJEMNOŚCI W LASERZE O EMISJI POWIERZCHNIOWEJ Z PIONOWĄ WNEKĄ REZONANSOWĄ

Streszczenie

W oparciu o model impedancji i stałych czasowych modulacji dla laserów o emisji powierzchniowej z pionową wnęką rezonansową (VCSEL) badamy opory i pojemności równoważnego obwodu w funkcji prądu przepływającego przez laser. Obserwujemy, że wraz ze wzrostem prądu przepływającego przez urządzenie, niektóre ze składowych rezystancji i pojemności w elektrycznym układzie zastępczym ulegają zmniejszeniu. Wraz ze wzrostem prądu zmniejsza się również stała czasu modulacji.